Density-functional approach to second-harmonic generation at metal surfaces

M. Weber and A. Liebsch
Institut für Festkörperforschung, Kernforschungsanlage Jülich, D-5170 Jülich, West Germany
(Received 23 October 1986)

Using density-functional theory we have determined the longitudinal second-harmonic response of various simple-metal surfaces in the limit of small frequencies. The metal is described by the semi-infinite jellium model and the electron distributions in the absence and in the presence of the external field are calculated self-consistently using the local-density approximation. Previous theoretical estimates of the normal component of the surface current density were based on the free-electron or the hydrodynamic model which do not adequately describe the detailed behavior of the electronic density in the vicinity of the surface. We find that, at low frequencies, the longitudinal surface current is proportional to the static second-order polarization whose integrated weight is given by the first moment of the second-order induced density. The centroid of the second-order polarization lies about 0.5 Bohr radii farther away from the positive background edge than the static image plane. Its integrated weight is 1—2 orders of magnitude larger than in the hydrodynamic model. Correspondingly, the a parameter, which had been introduced by Rudnick and Stern as a measure of the longitudinal second-harmonic response, is also significantly larger than its hydrodynamic value.

I. INTRODUCTION

There has been a recent resurgence of interest in the second-harmonic generation (SHG) of light at metal surfaces because of its demonstrated utility as a surface probe.[1] The second-harmonic current present near a metal surface consists of three parts: a "bulk" current which extends about an optical skin depth into the metal, and two surface currents (parallel and perpendicular to the surface) which extend only a few angstroms into the metal.[2] The nonlinear surface current most sensitive to the details of the surface charge distribution, and hence most interesting to calculate quantitatively, is the longitudinal surface current which flows normal to the surface.

Theoretical work on the second-harmonic response of metal surfaces has been until now treated only within the free-electron model or the hydrodynamic model, both of which, as pointed out by a number of authors,[2–8] are too crude to give a quantitative description of electron behavior near surfaces. The most serious drawback of these models is that the electron distribution of the metal is assumed to be constant up to the plane of the surface and to fall abruptly to zero at this plane. In a quantum-mechanical description, of course, the density must vary continuously in the region of the metal-vacuum interface.

In the present work, the density-functional approach is used to calculate the second-harmonic response of a semi-infinite metal to a low-frequency uniform electric field oriented perpendicular to the surface. Since we are primarily interested in the response at simple-metal surfaces, the ionic potential is treated within the jellium model. The free-electron-like aspects of the noble-metal conduction electrons should also be represented adequately by this model. Electron-electron interactions are described within the local-density approximation (LDA) of exchange and correlation. Thus, in contrast to the previously employed free-electron and hydrodynamic calculations, the smoothness of the electron distribution in the surface region, the Friedel oscillations in the interior of the metal, as well as the exponential tails in the vacuum are fully taken into account.

The theory presented below is intended to describe the normal component of the surface current at very low frequencies. In this limit, the longitudinal surface current is linear in ω and the constant of proportionality is directly related to the second-harmonic polarization. Since this polarization is nearly independent of ω near the static limit, we derive it from the nonlinear electron density induced at the metal-vacuum interface by a purely static electric field oriented perpendicular to the surface. The recent hydrodynamic results of Corvi and Schaich[8] showed that the a parameter, which is a measure of the normal component of the second-harmonic polarization, at low frequencies does not differ much from its value in the static limit. If we assume that this qualitative behavior also holds in more realistic response theories, then our results can be expected to be representative of the longitudinal second-harmonic response for frequencies $\omega \lesssim 0.1\omega_p$ where ω_p is the bulk plasma frequency.

We find that the second-harmonic polarization is largest in the tails of the equilibrium electron distribution. In general, its spatial shape is similar to that of the linearly induced density, but it is shifted farther out into the vacuum. Typically, the centroid lies about $0.5a_0$ (Bohr radius) farther away from the edge of the positive background than the static image plane. The integrated weight of the second-harmonic polarization is found to be about 1 to 2 orders of magnitude larger than in the hydrodynamic model and, in addition, to vary quite differently with the bulk density $\bar{n}$. As a consequence, the a parameter ob-

tained from the density-functional response treatment also differs significantly from its hydrodynamic value. For bulk densities specified by $r_s=2$, 3, 4, and 5 ($r_s=[3/(4\pi\bar{n})]^{1/3}$) we find $a=-28.4$, -12.9, -8.6, and -7.4, respectively. In contrast, in the low-frequency limit, the single-step hydrodynamic model gives $a=-\frac{2}{9}$ independently of the bulk electronic density.[9] If the electronic density at the surface is assumed to consist of more than one step, however, hydrodynamic theory can give much larger absolute values of a.[9] These results clearly demonstrate the need of a proper quantum-mechanical description of the electron distribution in the surface region.

II. THEORY

To determine the ground-state electronic properties of the semi-infinite metal we use the density-functional formalism[10] which, in principle, yields the exact electron density of the interacting many-particle system. In practice, the local-density approximation (LDA) is usually made, which leads to a local exchange-correlation potential. Here, the same potential is used as in the work by Lang and Kohn[11] (Wigner interpolation formula).

In order to describe the response of the semi-infinite electron gas to a finite-frequency external electromagnetic field the time-dependent extension of the density-functional approach,[12] which has recently been applied to determine the dynamical response of a variety of systems,[12–14] could be used. The nonlinear optical response of atoms has also been calculated using this approach.[15] However, at small real frequencies and long wavelengths, stable solutions of the response of a semi-infinite metal seem difficult to achieve. We therefore propose here a different procedure which relies principally on the static response properties of the metal, but which nevertheless should give qualitatively correct results for the longitudinal response in the limit of small frequencies.

In the presence of a static external electric field E oriented perpendicular to the surface, the electron density may be expanded as follows:

$$n(z)=n_0(z)+En_1(z)+E^2n_2(z)+\cdots , \tag{1}$$

where $n_0(z)$ is the equilibrium density profile and the induced densities $n_i(z)$, $i\geq 1$, are independent of the external field strength E. Now, let us assume that the uniform applied field has a time dependence of the form

$$E(t)=E_0\sin(\omega t) . \tag{2}$$

If the frequency ω is sufficiently small, we may assume that the electronic density responds adiabatically to this time-dependent field, i.e., the time-dependent density $n(z,t)$ has a similar expansion as in (1), with E replaced by $E(t)$,

$$n(z,t)=n_0(z)+E(t)n_1(z)+E^2(t)n_2(z)+\cdots . \tag{3}$$

Using (2) and trigonometric identities, this expression may be rewritten as

$$\begin{aligned} n(z,t)=&[n_0(z)+\tfrac{1}{2}E_0^2n_2(z)+\tfrac{3}{8}E_0^4n_4(z)+\cdots]+[E_0n_1(z)+\tfrac{3}{4}E_0^3n_3(z)+\cdots]\sin(\omega t)\\ &+[-\tfrac{1}{2}E_0^2n_2(z)-\tfrac{1}{2}E_0^4n_4(z)+\cdots]\cos(2\omega t)+[-\tfrac{1}{4}E_0^3n_3(z)+\cdots]\sin(3\omega t)+[\tfrac{1}{8}E_0^4n_4(z)+\cdots]\cos(4\omega t)+\cdots . \end{aligned} \tag{4}$$

This series is now in the proper form for comparison with a Fourier expansion (leaving out terms which vanish identically),

$$\begin{aligned} n(z,t)=&n_{\rm dc}(z)+n_\omega(z)\sin(\omega t)+n_{2\omega}(z)\cos(2\omega t)\\ &+n_{3\omega}(z)\sin(3\omega t)+n_{4\omega}(z)\cos(4\omega t)+\cdots , \end{aligned} \tag{5}$$

where $n_{\rm dc}(z)$ is the *time*-independent part of the density, not to be confused with the *field*-independent equilibrium distribution $n_0(z)$. Focusing on the second-harmonic contribution, we find

$$n_{2\omega}(z)=-\tfrac{1}{2}E_0^2n_2(z)+O(E_0^4) . \tag{6}$$

Thus, we have established a direct connection between the static second-*order* density and the low-frequency second-*harmonic* density.

According to Eqs. (4) and (5), the time-dependent terms of the density are in the adiabatic limit given by the density components induced by a static electric field. We calculate the first-and second-order contributions $n_1(z)$ and $n_2(z)$ by solving the density-functional equations for the semi-infinite jellium system in the presence of the external potential $\phi_{\rm ext}(z)=\pm eE_0z$.[16] Thus, the linearly induced density $n_1(z)$ is the same as that obtained previously by Lang and Kohn.[11] Its centroid defines the static image plane. The main quantity of interest in the present work is the second-order density $n_2(z)$ whose spatial distribution and overall size determine the second-harmonic response in the low-frequency limit.

In order to obtain the current density from the time-dependent density, we use the continuity equation ($e<0$)

$$\nabla\cdot\mathbf{j}(\mathbf{r},t)+\frac{\partial}{\partial t}en(\mathbf{r},t)=0 \tag{7}$$

with the boundary condition of zero current far from the surface. Of course, at finite frequencies, there will always be a tangential electric field which, in turn, leads to a current parallel to the surface. Thus, knowledge of $n(\mathbf{r},t)$ does not give one full knowledge of both parallel and perpendicular components of $\mathbf{j}(\mathbf{r},t)$. However, since the tangential component of the electric field at the surface of a metal vanishes in the static limit, we neglect the transverse current and replace Eq. (7) by

$$\frac{\partial}{\partial z}j_\perp(z,t)+\frac{\partial}{\partial t}en(z,t)=0 . \tag{8}$$

Support for the validity of this approximation comes from the results obtained by Corvi and Schaich[8] for the hydrodynamic model: At low frequencies, the a parameter is nearly independent of the angle of incidence of a p-polarized electromagnetic wave and its magnitude is determined by its value in the static limit. We expect this qualitative behavior to hold also in more refined dynamic response theories, i.e., the static second-order density is the central quantity which governs the longitudinal second-harmonic response at frequencies up to about $0.1\omega_p$.

III. RESULTS AND DISCUSSION

Figure 1 summarizes our results for the second-order densities induced at several metal surfaces by a uniform static electric field. Shown is the polarization ($\nabla\cdot\mathbf{P}=n$, $e=-1$),

$$P_2(z)=\int_{-\infty}^{z} dz' n_2(z')=-\int_{z}^{\infty} dz' n_2(z') , \tag{9}$$

together with the equilibrium densities $n_0(z)$ and the linearly induced densities $n_1(z)$. The functions $n_1(z)$ and $n_2(z)$ were obtained from a calculation of the self-consistent density for a semiinfinite metal with a slight positive or negative surface charge σ. Denoting these densities by $n_+(z)$ and $n_-(z)$, respectively, and using the expansion

$$n(z)=n_0(z)+\sigma n_1(z)+\sigma^2 n_2(z)+\cdots , \tag{10}$$

one has

$$n_1(z)=\frac{1}{2\sigma}[n_+(z)-n_-(z)] , \tag{11}$$

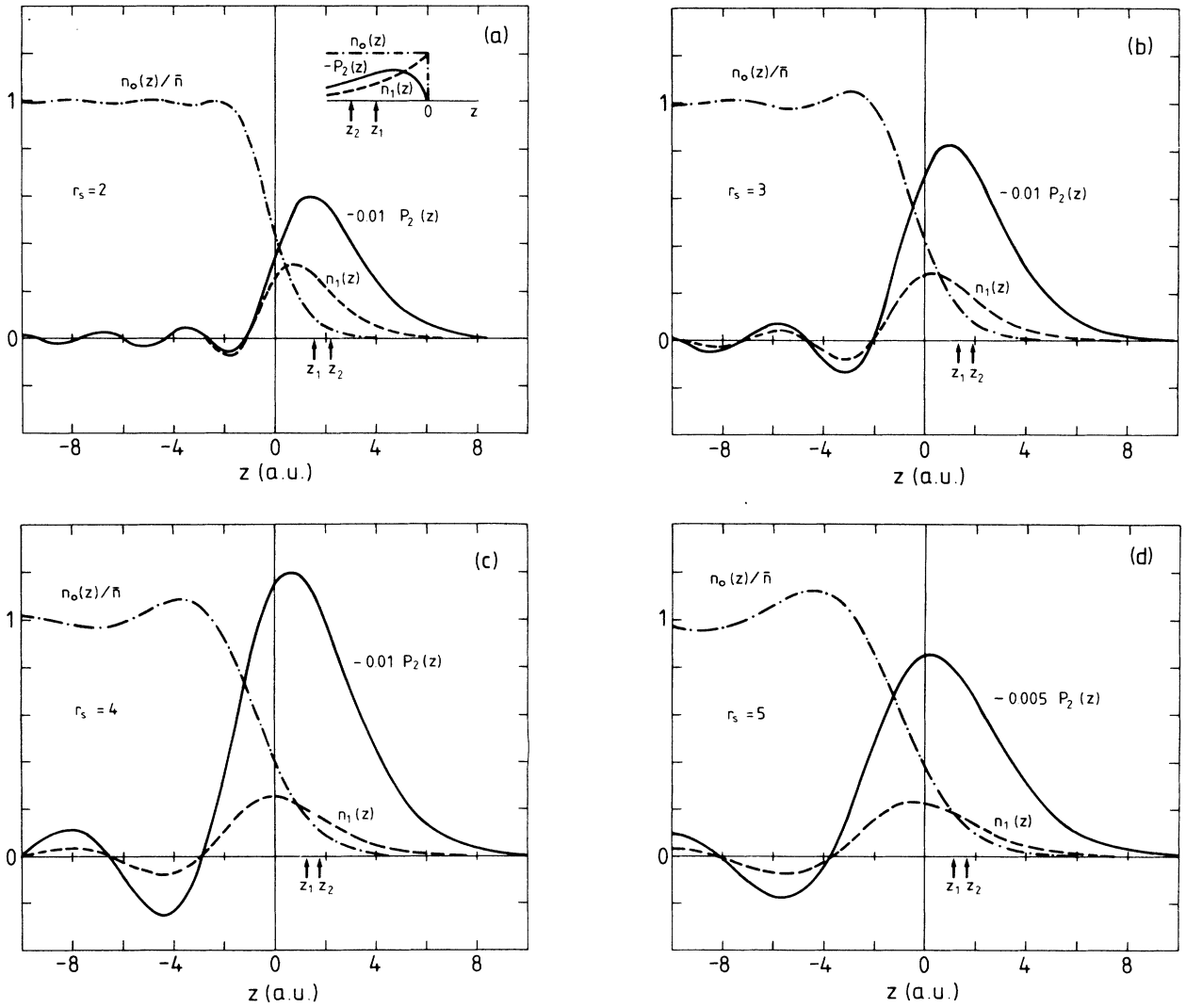

FIG. 1. Second-order polarization $P_2(z)$, Eq. (9) (solid line) and first-order density $n_1(z)$ (dashed line) induced at four metal surfaces by static uniform electric field. The normalized equilibrium profile, $n_0(z)/\bar{n}$, is shown by the dot-dashed line. The arrows indicate the centroid positions, z_1 and z_2, Eqs. (14) and (15), of $n_1(z)$ and $P_2(z)$, respectively. Inset: qualitative form of corresponding quantities in the hydrodynamic model.

$$n_2(z)=\frac{1}{2\sigma^2}[n_+(z)+n_-(z)-2n_0(z)] . \quad (12)$$

In the numerical calculations, the actual values of σ were of the order of 10^{-4} a.u. The linear-induced density $n_1(z)$ in Fig. 1 is normalized to unity:

$$\int_{-\infty}^{\infty} dz\, n_1(z)=1 . \quad (13)$$

Thus the centroid of $n_1(z)$ is

$$z_1=\int_{-\infty}^{\infty} dz\, z n_1(z) , \quad (14)$$

while that of $P_2(z)$ is given by

$$z_2=\int_{-\infty}^{\infty} dz\, zP_2(z)\Big/\int_{-\infty}^{\infty} dz\, P_2(z) = \tfrac{1}{2}\int_{-\infty}^{\infty} dz\, z^2 n_2(z)\Big/\int_{-\infty}^{\infty} dz\, z n_2(z) . \quad (15)$$

In Eqs. (9) and (15), we have made use of the fact that

$$\int_{-\infty}^{\infty} dz\, n_2(z)=0 . \quad (16)$$

The numerical values of z_1 and z_2 are given in Table I together with the widths γ_1 and γ_2 [full width at half maximum (FWHM)] of $n_1(z)$ and $P_2(z)$, respectively. Also given is the integrated weight of $P_2(z)$ which is determined by the first moment of $n_2(z)$,

$$p_2\equiv\int_{-\infty}^{\infty} dz\, P_2(z)=-\int_{-\infty}^{\infty} dz\, z n_2(z) . \quad (17)$$

From the continuity equation (8) and the relation (4) we see that the spatial distribution of the longitudinal second-harmonic current is directly proportional to the second-order polarization defined in Eq. (9):

$$j_{2\omega}(z)=\omega E_0^2 P_2(z)/(4\pi)^2 . \quad (18)$$

Thus, the polarization curves shown in Fig. 1 give a direct picture of the shape of the normal surface current and of its location with respect to the surface. Our results demonstrate that the longitudinal second-harmonic current is concentrated predominantly outside the ionic background. Its shape as a function of z is similar to that of the linearly induced density $n_1(z)$. However, its width tends to be somewhat larger than that of $n_1(z)$ and its center of gravity, z_2, typically lies about $0.5a_0$ farther from the jellium edge than z_1. (Note that the jellium edge lies at a distance $d/2$ outside the outermost plane of nuclei where d specifies the spacing of atomic planes parallel to the surface.) Furthermore, the integrated strength of the normal surface current is, in the low-frequency limit, directly proportional to the first moment of the static second-order-induced density.

TABLE I. First- and second-order response properties of various simple-metal surfaces: centroids, z_1 and z_2, of linear-induced density $n_1(z)$ and of second-order polarization $P_2(z)$, respectively [see Eqs. (14) and (15)]. The widths (FWHM) of these distributions are γ_1 and γ_2. The integrated weights of the second-order polarizations in the density-functional approach and in the hydrodynamic model are p_2 and $p_2^{\rm hd}$, respectively [see Eqs. (17) and (24)]. The density-functional value for the a parameter is obtained from Eq. (25). In the hydrodynamic model $a=-\frac{2}{9}$ independent of r_s [see Eq. (27)]. (All values are in atomic units.)

r_s	2	3	4	5
z_1	1.57	1.35	1.25	1.17
z_2	2.18	1.92	1.77	1.70
γ_1	3.0	3.6	4.2	4.7
γ_2	3.8	4.3	4.9	5.5
$-p_2$	239	365	579	970
$-p_2^{\rm hd}$	1.9	6.3	14.9	29.1
$-a$	28.4	12.9	8.6	7.4

Since most of the previous calculations of the second-harmonic response at metal surfaces were based on the hydrodynamic model, it is of interest to compare its predictions for the induced densities with the results presented above. In the static limit, it is straightforward to calculate $n_1(z)$ and $n_2(z)$ analytically in the hydrodynamic case for a uniform electric field perpendicular to the surface.[9] If the ground-state profile is taken to be

$$n_0(z)=\begin{cases}\bar{n} & \text{for } z\le 0 ,\\ 0 & \text{for } z>0 ,\end{cases} \quad (19)$$

the first- and second-order-induced densities are given by the expressions

$$n_1(z)=ke^{kz} , \quad (20)$$

$$n_2(z)=\frac{k^2}{9\bar{n}}(2e^{2kz}-e^{kz}) \quad (21)$$

for $z\le 0$ and $n_1(z)=n_2(z)=0$ for $z>0$. The second-order polarization then has the form

$$P_2(z)=\frac{k}{9\bar{n}}(e^{2kz}-e^{kz}) . \quad (22)$$

The parameter k in these expressions is defined by

$$k^2=\frac{4\pi e^2\bar{n}^{1/3}}{5\xi/3} , \quad (23)$$

where the constant ξ relates electron density and pressure in the hydrodynamic theory, i.e., $p=\xi n^{5/3}$.

The functions $n_1(z)$ and $P_2(z)$ are sketched in the inset of Fig. 1(a). The centroids of these quantities are located at $z_1=-1/k$ and $z_2=-1.5/k$, respectively. Thus, in contrast to the density-functional results, the centroid of $P_2(z)$ actually lies deeper inside the metal than that of $n_1(z)$. Moreover, the integrated weight of $P_2(z)$ is

$$p_2^{\rm hd}=\int_{-\infty}^{0} dz\, P_2(z)=(-18\bar{n})^{-1} . \quad (24)$$

For the four bulk densities specified by $r_s=2$, 3, 4, and 5, these values are given in Table I. They tend to be 1 to 2 orders of magnitude smaller than the density-functional values. They also exhibit a rather different dependence on the bulk density $\bar{n}$.

Having determined the second-order polarization, we are now able to make contact with the dimensionless parameter a which was introduced by Rudnick and Stern[2] as a measure of the longitudinal part of the second-harmonic surface current. According to Eq. (29) of Ref. 8 [see also Eq. (3.3) of Ref. 3], at low frequencies a is given by (atomic units),

$$a = 4\bar{n} \int_{-\infty}^{\infty} dz\, P_2(z) = 4\bar{n} p_2 \ , \tag{25}$$

where the Drude dielectric function has been used to determine the electric field in the interior of the metal. Thus, at low frequencies, the parameter a is a direct measure of the integrated weight of the static second-order polarization induced at the metal surface. Using Eq. (18), we may express a in terms of the longitudinal second-harmonic current

$$a = (4\pi)^2 \frac{4\bar{n}}{\omega E_0^2} \int dz\, j_{2\omega}(z) \ . \tag{26}$$

From the density-functional results for p_2 in Eq. (25), we obtain for a the values given in Table I. These values are considerably larger than the hydrodynamic result which, according to Eq. (24), is[9]

$$a^{\rm hd} = 4\bar{n} p_2^{\rm hd} = -\tfrac{2}{9} \tag{27}$$

independently of the bulk density. It should be recalled, however, that this hydrodynamic value refers to an equilibrium electron density which drops abruptly from its bulk value to zero. If the density profile is modeled, on the other hand, by a two-step profile, a is approximately given by[9]

$$a \approx -2/(9f) \ , \tag{28}$$

where f is the average fractional charge density over the range near the surface where the screening of the applied field takes place.

The large values of a which we obtain from density-functional theory are consistent with a recent qualitative argument by Sipe *et al.*[3] Using the hydrodynamic model, they take into account the fact that the electrons producing the longitudinal second-harmonic current may have a local "effective plasma frequency" ω_0. Writing

$$a = -2(\omega_p^2 - 4\omega^2)/(\omega_0^2 - 4\omega^2) \ , \tag{29}$$

they find at low frequencies

$$a = -2\omega_p^2/\omega_0^2 = -2\bar{n}/\bar{n}_0 \ , \tag{30}$$

where we have related ω_0 to a local effective density $\bar{n}_0$ via $\omega_0^2 = 4\pi\bar{n}_0$. Thus, with a taking on the values given in Table I, we obtain the following for $r_s = 2,3,4,5$: $\bar{n}_0/\bar{n} = 0.07$, 0.16, 0.23, and 0.27, respectively. This trend is quite consistent with the fact that the maxima of the second-harmonic polarizations shown in Fig. 1 are located at distances from the jellium edge where the equilibrium density has dropped to about 11%, 20%, 27%, and 33% of their bulk values (for $r_s = 2$, 3, 4, and 5).

IV. CONCLUSION

We have presented a calculation of second-harmonic generation at various simple-metal surfaces using density-functional theory. In contrast to previously employed free-electron and hydrodynamic models our quantum-mechanical treatment takes the profile of the equilibrium electron density at the surface and its nonlocal response to the external fields fully into account. We have shown that at low frequencies the longitudinal part of the second-harmonic current can be obtained from the nonlinear density induced by a static electric field.

Our results demonstrate that this current is located predominantly in the exponential tail of the equilibrium density and that the second-harmonic signal should therefore be very sensitive to surface conditions. This is consistent with experiments which have shown that the presence of small fractions of adsorbed monolayers can be detected using this technique. We also find that the overall size of the longitudinal SH response is 1 to 2 orders of magnitude larger than predicted by hydrodynamic calculations based on a single-step density profile. In particular, for the a parameter we obtain values between ~ -28 ($r_s = 2$) and -7 ($r_s = 5$), whereas hydrodynamic theory gives $a = -\frac{2}{9}$ independently of the bulk density.

Since the a parameter in the present work is obtained from a purely static response calculation, the only remaining approximation in the problem is related to the treatment of electron-electron interactions. In principle, the density-functional approach yields an exact quantum-mechanical description of ground-state properties such as the profile of the electronic density. In practice, however, the true exchange-correlation functional is replaced by a local functional. As a result, the surface potential falls off exponentially in the vacuum instead of having image-like behavior. Since the second-harmonic polarization is located predominantly in the tails of the ground-state electron profile, its shape and magnitude might also be influenced by the local approximation. This effect would become larger with growing r_s because of the greater importance of exchange and correlation in low-density systems. On the other hand, the discrepancy between the hydrodynamic value of a and the density-functional result gets larger towards higher bulk densities. This discrepancy should therefore not be a consequence of the local exchange-correlation functional.

Recent measurements on Al and Ag films deposited on Glass prisms were interpreted by Quail and Simon[17] within the hydrodynamic model by Sipe *et al.*[3] At a frequency $\omega = 1.17$ eV they achieve a fairly consistent fit of the angle dependence of the SH reflection for $a \approx 1.5$ (Al, $r_s \approx 2$) and $a \approx 0.9$ (Ag, $r_s \approx 3$). While these values are much larger than the actual hydrodynamic value at low frequencies, they are also much smaller than our density-functional results. It is not clear, however, whether the metal-glass interface at which most of the SHG takes place in this experiment is well represented by our metal-vacuum interface. Thus, we are hesitant to claim that these data contradict our theoretical predictions. It would be of great interest to have SHG performed on single-crystal metal surfaces prepared under ultrahigh vacuum conditions.

ACKNOWLEDGMENTS

We thank Professor W. L. Schaich for permission to quote the hydrodynamic results in the static limit. One of us (M.G.W.) would like to thank the Alexander von Humboldt Foundation whose support made this collaboration possible.

[1]T. F. Heinz, H. W. K. Tom, and Y. R. Shen, Laser Focus **19**, 101 (1983); Y. R. Shen, J. Vac. Sci. Technol. B **3**, 1464 (1985).
[2]J. Rudnick and E. A. Stern, Phys. Rev. B **4**, 4274 (1971).
[3]J. E. Sipe, V. C. Y. So, M. Fukui, and G. I. Stegemann, Phys. Rev. B **21**, 4389 (1980).
[4]C. S. Wang, J. M. Chen, and J. R. Bower, Opt. Commun. **8**, 275 (1973).
[5]J. R. Bower, Phys. Rev. B **14**, 2427 (1976).
[6]A. Griffin and H. Kranz, Phys. Rev. B **14**, 5068 (1977).
[7]J. Rudnick and E. A. Stern, in *Polaritons,* edited by E. Burstein and F. De Martini (Plenum, New York, 1974).
[8]M. Corvi and W. L. Schaich, Phys. Rev. B **33**, 3688 (1986).
[9]W. L. Schaich (private communication).
[10]P. Hohenberg and W. Kohn, Phys. Rev. **136**, B864 (1964); W. Kohn and L. J. Sham, *ibid.* **140**, A1133 (1965).
[11]N. D. Lang and W. Kohn, Phys. Rev. B **1**, 4555 (1970); **7**, 3541 (1973).
[12]A. Zangwill and P. Soven, Phys. Rev. A **21**, 1561 (1980).
[13]M. J. Stott and E. Zaremba, Phys. Rev. A **21**, 12 (1980); J. F. Dobson and J. H. Rose, J. Phys. C **15**, 7429 (1980); W. Ekardt, Phys. Rev. Lett. **52**, 1925 (1984); A. G. Eguiluz, Phys. Rev. B **31**, 3303 (1985); A. Liebsch, *ibid.* **33**, 7249 (1986).
[14]P. J. Feibelman, Progr. Surf. Sci. **12**, 287 (1982), and references therein. (Note that in this work, the linear optical response is treated within the random-phase approximation rather than the time-dependent local-density approximation.)
[15]A. Zangwill, J. Chem. Phys. **78**, 5926 (1983).
[16]Nonlinear static response properties of jellium slabs were investigated by P. Gies and R. R. Gerhardts, Phys. Rev. B **31**, 6843 (1985).
[17]J. C. Quail and H. J. Simon, Phys. Rev. B **31**, 4900 (1985).